Chemistry & Biology
Article

Examination of the Role of Intestinal Fatty Acid-Binding Protein in Drug Absorption Using a Parallel Artificial Membrane Permeability Assay

Tony Velkov,[1] James Horne,[1] Aisha Laguerre,[1] Eric Jones,[1,3] Martin J. Scanlon,[1] and Christopher J.H. Porter[2,*]
[1] Department of Medicinal Chemistry
[2] Department of Pharmaceutics
Victorian College of Pharmacy, Monash University, Parkville, Victoria 3052, Australia
[3] Present address: Avexa Ltd., 576 Swan Street, Richmond, Victoria 3121, Australia.
*Correspondence: chris.porter@vcp.monash.edu.au
DOI 10.1016/j.chembiol.2007.03.009

SUMMARY

Transcellular diffusion across the absorptive epithelial cells (enterocytes) of the small intestine is the main route of absorption for most orally administered drugs. The process by which lipophilic compounds transverse the aqueous environment of the cytoplasm, however, remains poorly defined. In the present study, we have identified a structurally diverse group of lipophilic drugs that display low micromolar binding affinities for a cytosolic lipid-binding protein—intestinal fatty acid-binding protein (I-FABP). Binding to I-FABP significantly enhanced the transport of lipophilic drug molecules across a model membrane, and the degree of transport enhancement was related to both drug lipophilicity and I-FABP binding affinity. These data suggest that intracellular lipid-binding proteins such as I-FABP may enhance the membrane transport of lipophilic xenobiotics and facilitate drug access to the enterocyte cytoplasm and cytoplasmic organelles.

INTRODUCTION

Intracellular lipid-binding proteins (iLBPs) are a diverse family of low-molecular weight (12–15 kDa) cytosolic proteins [1, 2]. The fatty acid-binding protein (FABP) subfamily of iLBPs is of particular interest since, in many cells, FABPs are the most abundant proteins and may constitute as much as ~3%–6% of the cytosolic protein [1, 3]. While FABPs show distinctive tissue and cellular distribution patterns, it is not uncommon for FABPs to be expressed in multiple tissue types, and in the enterocyte both intestinal (I)-FABP and liver (L)-FABP are present in relatively high concentrations [3, 4].

Cytosolic FABPs display a common tertiary structure. Their consensus topology consists of two β sheets, which form a ''clam-like'' structure that encloses a large solvated cavity and is capped by a helix-turn-helix motif [2]. It is thought that the α-helical region acts as a ''dynamic portal,'' which opens to allow ligand entry to the binding cavity and then interacts with the bound ligand to cap the cavity opening [5–7]. All FABPs bind long-chain fatty acids (FAs); however, the stoichiometry of binding varies among the different members of the family. I-FABP, for example, binds FAs in a 1:1 stoichiometric ratio, while L-FABP binds two FAs in what appears to be an interdependent manner [5–8].

Despite extensive study, the precise physiological role of FABPs remains enigmatic. While a role in the intracellular trafficking of long-chain FAs is clear [1, 2, 9, 10], FABPs also bind non-FA ligands, including heme, eicosanoids, and xenobiotics [9, 11, 12], albeit with a markedly lower affinity. The biological significance of these lower-affinity binding interactions is not well understood. However, the concentration of FABPs in the enterocyte far exceeds the concentration of free FAs [1, 3], and significant quantities of FABP are likely to be available for binding these other ligands, even in the presence of endogenous FAs.

For orally administered drugs, passage across the enterocyte is a potential barrier to effective absorption [13, 14]. Historically, attention has focused on the interaction of drugs with membrane transporters located on either the apical or basolateral membrane of the enterocyte [15]. In contrast, drug transport from the apical enterocyte membrane into the cytoplasm, diffusion across the cytoplasm, and subsequent access to the basolateral membrane have been almost entirely neglected. In this respect, transport across the primarily aqueous cytoplasm is expected to be most problematic for poorly water-soluble, lipophilic molecules. In a recent report, evidence for the binding of a limited number of non-FA lipophilic drugs to I-FABP was established, suggesting that I-FABP could serve as a water-soluble drug carrier in the enterocyte [11]. In the present communication, those findings have been expanded to provide definitive data describing the binding of several homologous series of drug molecules to I-FABP. From these data, indications of structure-binding relationships between drug molecules and I-FABP have been inferred. Data reflecting the likely passive transport processes at the apical and basolateral membrane domains of the enterocyte have been generated by using

Table 1. Binding Affinity of I-FABP for Different Series of Structurally Related Compounds as Determined Fluorometrically by Displacement of ANS

Ligand	K_i[a] (μM) (Mean ± SD, n = 3)	K_i[b] (μM) (Mean ± SD, n = 3)	Log $D_{pH\ 7.4}$
Fatty Acids			
Myristic acid (14:0)	0.041 ± 0.002	0.061 ± 0.004	3.48
Palmitic acid (16:0)	0.024 ± 0.001	0.038 ± 0.001	4.54
Fenamates			
Tolfenamic acid	2.8 ± 0.7	7.2 ± 0.9	2.32
Flufenamic acid	3.7 ± 0.8	10.9 ± 1.8	2.03
Meclofenamic acid	8.9 ± 2.0	21 ± 5.3	2.27
Mefenamic acid	63 ± 10	110 ± 18	1.77
Diclofenac	150 ± 9.6	520 ± 11	0.11
Propionic Acid Derivatives			
Fenoprofen	14 ± 0.5	64 ± 4.1	0.69
R-Flurbiprofen	15 ± 2.8	48 ± 3.1	0.92
(*R*/*S*)-Flurbiprofen	20 ± 2.3	70 ± 11	0.92
Ketoprofen	24 ± 3.0	74 ± 3.4	−0.31
S-Flurbiprofen	26 ± 1.1	67 ± 2.2	0.92
R-Ibuprofen	32 ± 4.2	64 ± 1.5	0.77
(*S*)-(-)-Naproxen	56 ± 4.2	180 ± 6.8	0.03
(*R*/*S*)-Ibuprofen	58 ± 8.4	100 ± 8.8	0.77
S-Ibuprofen	84 ± 2.5	150 ± 1.4	0.77
Indoprofen	130 ± 1.8	190 ± 0.3	−1.23
Nabumetone	NB[c]	NB[c]	2.82
Fibrates			
Fenofibric acid	1.0 ± 0.2	3.7 ± 0.1	−0.04
Ciprofibrate	24 ± 1.1	72 ± 3.5	−1.28
Bezafibrate	33 ± 0.7	100 ± 4.4	−0.17
Clofibric acid	52 ± 1.8	110 ± 9.4	−1.13
Naphthalene Derivatives			
bisANS	2.0 ± 0.5	5.6 ± 0.7	−2.19
ANS	3.2 ± 0.3	7.3 ± 0.2	−1.27
TNS	45 ± 10	130 ± 21	−0.81
Bridged Bi-Phenyl Compounds			
Benzyl salicylate	NB[c]	NB[c]	3.93
Pyrilamine	NB[c]	NB[c]	1.64
Phenytoin	NB[c]	NB[c]	2.47
Bifenox	NB[c]	NB[c]	5.79
Verapamil	NB[c]	NB[c]	3.4
Mepronil	NB[c]	NB[c]	4.12
N-Phenyl-2,3-xylidine	NB[c]	NB[c]	3.89
Other Mono-Carboxylic Acid Derivatives			
Acifluorfen	4.2 ± 1.2	8.9 ± 2.1	1.90
2-Naphthoxyacetic acid	7.2 ± 1.9	14 ± 3.6	−1.28

Table 1. *Continued*

Ligand	K_i[a] (μM) (Mean ± SD, n = 3)	K_i[b] (μM) (Mean ± SD, n = 3)	Log $D_{pH\ 7.4}$
1-Naphthaleneacetic acid	32 ± 5.7	60 ± 8.7	−0.33
Benzilic acid	110 ± 14	200 ± 24	−1.07
Jasmonic acid	140 ± 21	350 ± 30	−1.19
Valproate	240 ± 23	470 ± 22	0.15
Asprin	300 ± 11	460 ± 18	−2.51
Nalidixic acid	NB[c]	NB[c]	−2.86
Indole Acids			
Indole-3-butyric acid	72 ± 12	170 ± 16	−0.21
3-Indoleacetic acid	93 ± 16	200 ± 21	−1.21
Heteroaryl Acetic Acid Derivatives			
Tolmetin	1300 ± 80	2200 ± 94	−1.36
Ketorolac	1700 ± 110	2300 ± 120	−1.90
Steroids			
Progesterone	20 ± 4.6	32 ± 5.3	4.04
Prednisolone	95 ± 9.4	113 ± 10	1.69
Dexamethasone	1100 ± 109	1200 ± 130	2.06
Cortexolone	1600 ± 89	1900 ± 112	2.74
Benzodiazepines			
Diazepam	2000 ± 87	2200 ± 110	2.96
Nitrazepam	2000 ± 95	2300 ± 96	2.84
Lorazepam	2100 ± 92	2500 ± 105	2.48

[a] 20 mM Tris-HCl (pH 8.0) buffer.
[b] 50 mM Tris-HCl (pH 8.0), 150 mM NaCl buffer.
[c] NB, no binding detected.

artificial phospholipid membranes, and functional information describing the effects of a FABP on transmembrane drug transport is presented. Together, these data suggest a possible role for iLBPs in both facilitating drug transport across the enterocyte and regulating intracellular drug disposition.

RESULTS

Binding of I-FABP for Selected Lipophilic Drugs

The binding affinity of I-FABP for several series of lipophilic drugs is documented in Table 1 (and Figure S1; see the Supplemental Data available with this article online). The apparent octanol-water partition coefficient for each drug at pH 7.4 (log $D_{7.4}$) is shown as a measure of lipophilicity. In general, compounds containing a terminal carboxylate and an extended hydrophobic moiety showed the greatest binding affinity for I-FABP. The importance of the carboxylate is highlighted by comparing compounds, such as nabumetone (no significant binding) and naproxen (K_i = 56 μM), that differ principally in the presence or absence of the carboxylate functionality. An increase in K_i was also observed under high-salt buffer conditions, suggesting that ionic interactions are a significant factor in drug-I-FABP binding. The carboxylate group, however, is not an absolute requirement for binding, as demonstrated by certain steroids that show reasonable (albeit generally lower) binding affinities. Furthermore, a carboxylate group per se is not sufficient for binding, as several carboxylic acids were demonstrated not to bind.

The hydrophobic moiety is also important in determining binding affinity. For example, across the fenamates, propionic acid derivatives, and fibrates, there are compounds that differ primarily in the nature of the hydrophobic moiety, but that have binding affinities that differ by more than an order of magnitude. In general, compounds of similar size to the native FA ligands have the highest affinity. Compounds with shorter lipophilic chains (e.g., aspirin) or more bulky attachments (e.g., indoprofen) generally display lower affinities. Compounds in which the carboxylate is either absent or not at the terminus also display generally lower affinities. An exception to this trend is the naphthalene sulfonic acid series. However, we have previously shown that the binding mode of 1-anilino-8-naphthalene sulfonic acid (ANS) is somewhat different

than that of FAs and resembles the mode of binding previously observed for ANS and adipocyte lipid-binding protein (ALBP) [16].

Ligand-Induced Chemical-Shift Changes in I-FABP

To examine the binding of a range of drugs to I-FABP, a series of NMR chemical-shift perturbation experiments was undertaken. It has previously been shown that ligand binding results in perturbation of a large proportion of the ^{1}H-^{15}N crosspeaks in spectra of I-FABP [11, 17]. This is also the case in the current study, in which titration of each of the drugs resulted in perturbation of the majority of ^{1}H-^{15}N resonances (Figure S2). As such, precise interpretation of ^{1}H-^{15}N chemical-shift perturbations is problematic. In contrast, measurements of ^{13}C chemical-shift perturbations typically provide a more precise description of the binding site [18]. This has been demonstrated for I-FABP binding to its endogenous ligand, FA [17]; binding to palmitate results in significant perturbations in $^{13}C_{\alpha}$ and $^{13}C_{\beta}$ chemical shifts for residues that are located at the binding interface (Figure 1).

Palmitate binds to I-FABP with the carboxylate head group buried within the cavity, where it forms a salt bridge with Arg106 and H bonds with both Arg106 and Trp82 [19]. The methylene tail of the FA binds in a bent conformation within a concave crevice lined with aromatic and hydrophobic amino acids. The methyl terminus of the FA acyl chain makes van der Waals contacts with aromatic "capping" residues within the portal. A $^{13}C_{\alpha}$ and $^{13}C_{\beta}$ chemical-shift perturbation map for palmitate binding to I-FABP, based on the published data [17], demonstrates that the residues undergoing significant chemical-shift perturbations are located almost exclusively at the binding interface. In the present study, we have assigned $^{13}C_{\alpha}$ and $^{13}C_{\beta}$ chemical shifts for apo-I-FABP and for I-FABP complexes with fenofibric acid, clofibric acid, and tolfenamic acid. (Deposited at BioMagResBank with accession numbers 15082, 7356, 7357, and 7355.) The results of the chemical-shift perturbation experiments are presented in Figure 1, in which the residues undergoing significant perturbations are mapped onto the crystallographic structure of I-FABP. Also shown are the highest-scoring poses for each of the ligands docked into I-FABP.

In the docking solution for fenofibric acid, the terminal carboxylate interacts with residues at the bottom of the I-FABP binding cavity in a similar manner to FAs. The remainder of the fenofibric acid interacts with residues in the hydrophobic crevice and makes contacts with portal residues. This mode of binding is supported by the chemical-shift perturbation data. In contrast, both the docking solution and chemical-shift mapping data for clofibric acid and tolfenamic acid suggest a mode of binding distinct from that of FAs. Thus, for clofibric acid, the residues that undergo the most significant perturbations are clustered at the bottom of the cavity, with few changes being observed in either the hydrophobic crevice or the portal region. This supports the docking solution, which shows the terminal carboxylate of clofibric acid positioned at the bottom of the cavity. From this position, the smaller clofibric acid does not extend to the hydrophobic crevice or portal, and this is reflected in the lack of observed chemical-shift perturbations in these regions. For tolfenamic acid, the carboxylate functionality is attached directly to the benzene ring. As such, while the carboxylate is still capable of interacting with Arg106, the steric bulk of the benzene ring prevents the carboxylate from penetrating deeply into the I-FABP binding cavity. For FAs, fenofibric acid, and clofibric acid, the carboxylate interacts with Arg106 in a bidentate fashion, such that both carboxylate oxygens interact with the Arg106 guanidinium group. With tolfenamic acid, the interaction is monodentate, and only one of the carboxylate oxygens interacts with Arg106. This is reflected in the lack of chemical-shift perturbations observed at the bottom of the cavity for tolfenamic acid.

Impact of Drug-FABP Binding on Membrane Transport

To examine the hypothesis that iLBPs facilitate transport across the apical absorptive membrane of the enterocyte and into the cytosol, a parallel artificial membrane permeability assay (PAMPA) has been utilized to model absorption events at the apical and basolateral membrane domains. The PAMPA system consists of a multilamelar membrane supported on a filter disc that separates two aqueous domains (vide infra). The PAMPA model was validated by assessment of the permeability of two reference compounds (caffeine and mannitol) that do not bind I-FABP. The data obtained were consistent with the literature [14] and did not change regardless of the presence or absence of I-FABP (Tables 2 and 3).

The experimental PAMPA data were obtained by using protocols designed to reflect uptake across the apical membrane and transport across the basolateral membrane. To examine uptake across the apical membrane, transport buffer was used in the donor chamber, and the impact of either buffer or 0.33 mM I-FABP in the acceptor chamber was evaluated. The I-FABP concentration (0.33 mM) was chosen to resemble the cytosolic level of I-FABP in enterocytes [1, 3]. Transport across the basolateral membrane was examined by employing I-FABP in the donor (cytoplasmic) chamber and either buffer or 0.66 mM HSA in the acceptor chamber. The concentration of HSA in the acceptor chamber was chosen to reflect the albumin concentration in plasma [20]. In this way, the model PAMPA system provides for experimental flexibility that is not evident during examination of transport across, for example, a cell monolayer, where transport events across apical and basolateral membranes are necessarily aggregated.

In the experiments designed to reflect events across the apical membrane, the rate of membrane uptake was obtained from the rates of drug loss from the donor solution (Figure 2, left-hand panel). Apparent permeability coefficients generated from disappearance plots revealed little difference in the rate of uptake of the most lipophilic probes, i.e., oleic acid (log $D_{7.4}$ = 3.48), progesterone (log $D_{7.4}$ = 4.04), and diazepam (log $D_{7.4}$ = 2.96) (Table 2).

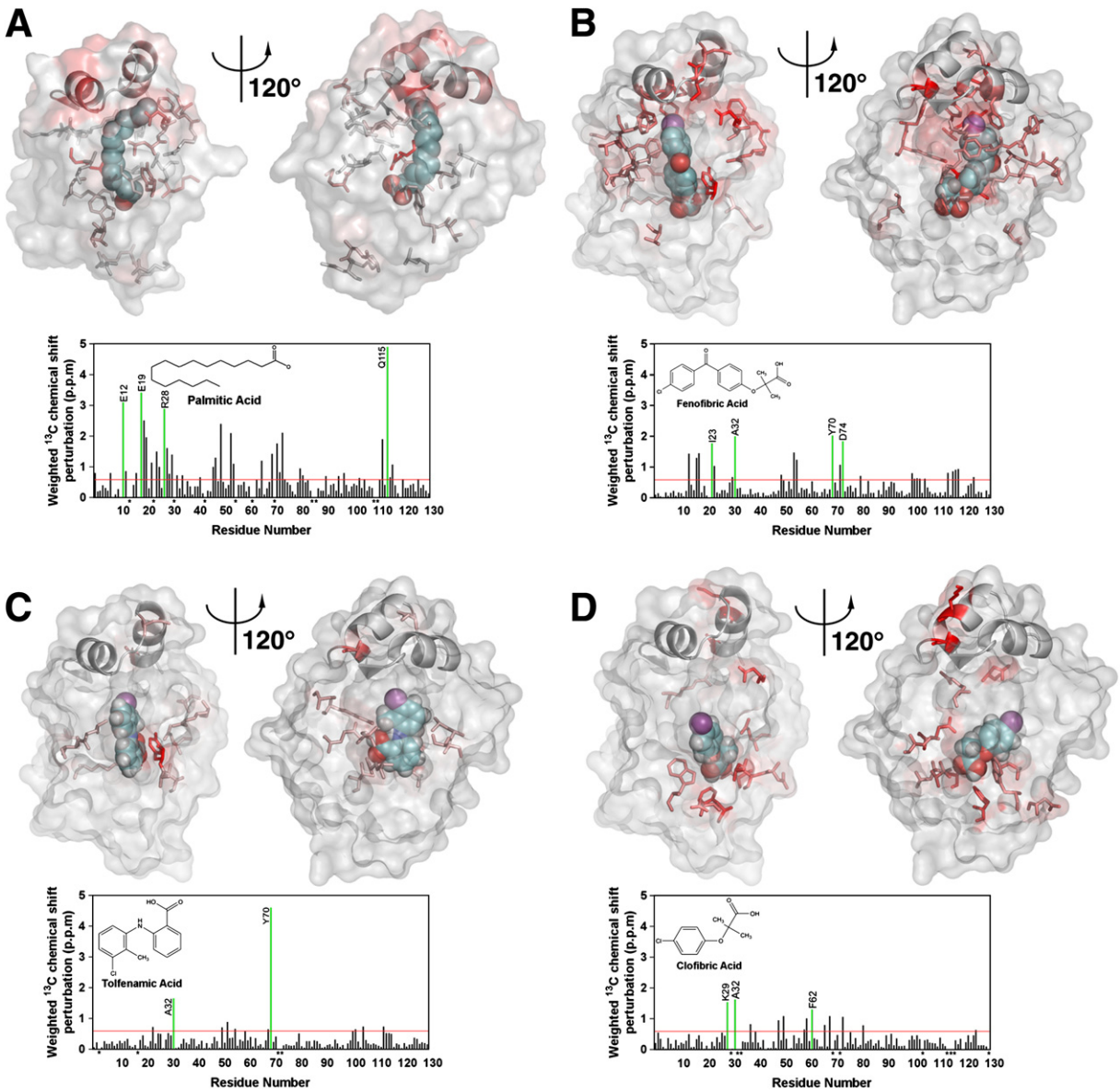

Figure 1. Chemical-Shift Perturbation Mapping of Ligand Binding to I-FABP

(A–D) Amino acids that displayed significant $^{13}C_{\alpha}$ and $^{13}C_{\beta}$ atom chemical-shift changes (>0.6 ppm) upon ligand binding were mapped onto the crystal structure of rat I-FABP. Perturbed residues are colored by using a linear ramp from white to red (minimal to highest perturbation). The molecular surface of the protein is depicted; the portal region is shown in ribbon representation. The two views are rotated by 120° about the y axis. The bottom panels show a plot of the $^{13}C_{\alpha}$ and $^{13}C_{\beta}$ chemical-shift changes upon ligand binding versus residue number. The >0.6 ppm threshold for a significant perturbation is shown as a red, horizontal line. The highly affected residues are shown as vertical, green bars. Stars indicate unassigned residues. (A) Chemical-shift perturbations induced by palmitic acid binding have been mapped onto the crystal structure of *holo*-palmitic acid-rat I-FABP (2IFB.pdb). (B–D) The crystal structure of *holo*-myristate-rat I-FABP (1ICM.pdb) was employed for the drug-docking models; the ligands (B) fenofibric acid, (C) tolfenamic acid, and (D) clofibric acid are shown in CPK representation in the position of the optimal docking solutions.

This is consistent with the general understanding that diffusion across the unstirred water layer (UWL) adjacent to the membrane surface is typically the rate-limiting step in the membrane permeation of highly lipophilic molecules [14, 21, 22]. Thus, the rates of diffusion of these small molecules across the UWL were high and similar in all cases [22]. In contrast, the rates of uptake of the less lipophilic probes, ibuprofen (log $D_{7.4}$ = 0.77), propranolol (log $D_{7.4}$ = 0.97), and tolfenamic acid, (log $D_{7.4}$ = 2.3), were lower, suggesting that uptake into the membrane was limited by membrane (as opposed to UWL) permeability.

For the more lipophilic compounds, the initial rate of disappearance from the donor chamber was nonlinear and markedly higher than the rate of appearance in the acceptor chamber. These differences reflect drug accumulation in the membrane (Figure 2, middle column). Closer

Table 2. Disappearance Kinetics Permeability Values Measured at pH 7.4 by the PAMPA Method

Donor/Acceptor	Buffer/Buffer	Buffer/I-FABP
Oleic acid	240 ± 11	240 ± 2.0
Tolfenamic acid	111 ± 25	101 ± 30
Progesterone	240 ± 26	270 ± 51
Ibuprofen	43 ± 6.9	50 ± 6.7
Diazepam	220 ± 10	200 ± 17
Propranolol	100 ± 14	100 ± 7.9
Caffeine	100 ± 3.0	100 ± 4.2
Mannitol	ND[a]	ND[a]

$P_e = 10^{-6}$ cm·s^{-1}. Mean ± SD, n = 3.
[a] ND, not detected.

inspection of the data in Figure 2 suggests that membrane retention was, as expected, related to drug lipophilicity and decreased across the series oleic acid ≈ progesterone > diazepam > tolfenamic acid > propranolol > ibuprofen. Drug concentrations in the membrane appeared to equilibrate after ~3 hr, after which time the rate of disappearance from the donor chamber approximated the rate of drug appearance in the acceptor chamber, indicating that conditions of steady-state drug transport had been attained (data not shown).

The presence of I-FABP in the acceptor chamber did not affect the kinetics of drug uptake into the membrane. In contrast, the rate of appearance of drug in the acceptor chamber was in some cases highly dependent on the presence of I-FABP. Thus, the transport of oleic acid, tolfenamic acid, progesterone, and, to a lesser extent, ibuprofen was significantly enhanced by the presence of I-FABP in the acceptor chamber (Table 3). Importantly, the degree of transport enhancement was also reflective of the relative drug binding affinity to I-FABP (Table 3; Table S1). For oleic acid and tolfenamic acid, the presence of I-FABP also reduced drug retention in the membrane and facilitated improved partitioning into the aqueous receptor compartment (Figure 2; Table S1). The impact of I-FABP in enhancing both the rate and extent of membrane transport is best exemplified by tolfenamic acid (K_i = 2.8 μM), although qualitatively similar events are evident with the lower-affinity ligands progesterone (K_i = 20 μM) and ibuprofen (K_i = 58 μM). Consistent with the very weak binding interaction between I-FABP and diazepam and the lack of interaction with propranolol, no significant differences in membrane retention or permeability were seen in the presence of I-FABP for these two probes.

In order to simulate drug permeation from the enterocyte cytosol across the basolateral membrane and into the underlying lamina propria, PAMPA assays were conducted with the inclusion of I-FABP (0.33 mM) in the donor chamber and HSA (0.66 mM) in the acceptor chamber. Under these conditions, oleic acid, tolfenamic acid, progesterone, and diazepam all showed enhanced appearance P_e values when compared to identical conditions but in the absence of albumin in the acceptor chamber (Table 3). In each case, the observed enhancement was dictated by drug lipophilicity and the relative binding affinities of each compound for HSA and I-FABP (Table 3). Drug binding to HSA promoted transport into the acceptor chamber, whereas drug binding to I-FABP in the donor chamber opposed this enhancement. Thus, no significant differences in transport were observed for the less lipophilic compounds ibuprofen and propranolol, and, in the case of oleic acid, the increase in transport resulting from HSA binding in the acceptor chamber was attenuated by similarly strong binding to I-FABP in the donor.

Table 3. Appearance Kinetics Permeability Values Measured at pH 7.4 by the PAMPA Method

Donor/ Acceptor	Buffer/ Buffer	Buffer/ I-FABP	I-FABP/ Buffer	I-FABP/ HSA	I-FABP Binding Affinity (K_i, μM)	HSA Binding Affinity (K_i, μM)	Effective Partition Coefficient (log $D_{pH7.4}$)
Oleic acid	1.2 ± 0.4	650 ± 29[a]	0.50 ± 0.1	9.2 ± 0.7[b]	0.056 ± 0.01	0.089 ± 0.01	3.48
Tolfenamic acid	8.1 ± 2.3	25.4 ± 3.2[a]	3.3 ± 1.4	7.4 ± 2.4[b]	2.8 ± 0.7	1.1 ± 0.5	2.32
Progesterone	32 ± 2.4	60 ± 5.4[a]	12 ± 1.3	190 ± 20[b]	20 ± 4.6	Site 1: 0.020 ± 0.006; Site 2: 30 ± 3.8	4.04
Ibuprofen	4.0 ± 0.8	6.3 ± 0.8[a]	3.3 ± 0.3	4.0 ± 0.5	58 ± 8.4	22 ± 4.3	0.77
Diazepam	36 ± 2.0	40 ± 5.5	25 ± 5.2	190 ± 15[b]	2000 ± 87	73 ± 8.4	2.96
Propranolol	24 ± 2.6	24 ± 1.2	24 ± 0.5	26 ± 0.4	NB[c]	66 ± 10.2	0.97
Caffeine	2.2 ± 0.1	2.2 ± 0.3	2.4 ± 0.1	2.4 ± 0.3	NB[c]	NB[c]	−0.24
Mannitol	ND[d]	ND[d]	ND[d]	ND[d]	NB[c]	NB[c]	−4.67

$P_e = 10^{-6}$ cm·s^{-1}. Mean ± SD, n = 3.
[a] Significantly larger than P_e obtained in the absence of I-FABP in the acceptor chamber ($p < 0.05$).
[b] Significantly larger than P_e obtained in the absence of HSA in the acceptor chamber ($p < 0.05$).
[c] NB, no binding detected.
[d] ND, not detected.

DISCUSSION

Recent advances in cell and structural biology have resulted in the identification of a wide range of transport proteins on the apical and basolateral membranes of enterocytes and have subsequently shown that these proteins can facilitate vectorial transport processes that either assist or impede (efflux) drug absorption. While considerable progress has therefore been made in the structural and functional characterization of transmembrane drug transporters, the role of cytosolic binding proteins in drug transport across the cell and intracellular drug transport to, for example, cytosolic sites of metabolism or translational signaling remains ill defined. In light of this, to our knowledge, the current study provides the first data linking specific structural details of drug binding to intracellular FA carrier proteins, such as I-FABP, with the potential impact on drug transport.

Notwithstanding their highly conserved tertiary structures, iLBPs can be divided into four subfamilies based on sequence homology and differences in ligand selectivity and binding geometries [23]. Subfamily I comprises the cellular retinoid-binding proteins in which a single ligand is typically bound near the cavity entrance under the double helix cap domain. The carboxylate of the ligand forms hydrogen bonds with highly conserved arginine and tyrosine residues within the ligand binding cavity. Subfamily II consists of L-FABP and the ileal bile acid-binding protein (I-BABP), which have two ligand-binding sites within the cavity. Both L-FABP and I-BABP are able to bind bulky ligands on account of their higher backbone flexibility and larger ligand entrance when compared to other iLBPs. Subfamily IV contains several different iLBP types, including heart, epidermal, and brain FABPs, which generally bind one FA in a U-shaped conformation. In structures of this subfamily, the carboxylate group of the FA is complexed by a network of hydrogen bonds with the side chains of the highly conserved cavity residues Arg106, Arg126, and Tyr128. I-FABP is the sole member of subfamily III, which is somewhat different from other iLBP subfamilies in the manner it binds FA [23]. I-FABP binds a single FA in an extended and slightly bent conformation [19, 23, 24]. Different FAs bind to I-FABP in very similar locations and orientations and differ principally in their interactions with residues located within the dynamic portal.

The binding interactions of I-FABP with its endogenous ligand (FA) have been widely reported [5–7, 17, 19, 23, 24]. While it has been known for some time that I-FABP is capable of interacting with non-FA ligands [25], there have been few studies characterizing its broader binding specificity. In the present study, we have characterized I-FABP binding to a range of lipophilic drugs. Detailed examination of the interaction of a range of compounds with I-FABP has allowed aspects of the drug binding specificity of the I-FABP binding cavity to be elucidated. The rank order of drug affinities observed can be rationalized in terms of the binding modes suggested by the NMR chemical-shift perturbations and the docking studies. These data suggest that each of the drugs binds within the cavity of I-FABP through a network of bonding interactions. Thus, fenofibric acid and tolfenamic acid appear to bind in somewhat different orientations—particularly with respect to the location of their carboxylate groups; however, their overall affinity is similar. In contrast, clofibric acid binds with its carboxylate group in a similar location to fenofibric acid and FA, but it is unable to access the hydrophobic groove and portal, which presumably contributes to its lower affinity. None of the drugs completely fill the binding cavity of I-FABP, suggesting that bulkier and structurally diverse ligands may be accommodated.

Binding and structural studies with an Arg106-Gln mutant of I-FABP have demonstrated that the ionic interaction is not essential for FA binding [19, 24]. In these studies, although FA affinity was reduced ~20 fold and the binding conformation was less well defined, FA was shown to bind the mutant FABP in a broadly similar conformation to the native protein [24]. Studies with the naturally occurring Ala54-Thr mutant human I-FABP have also indicated that the size of the portal residues appears to influence access to the binding cavity, although this did not greatly affect ligand binding affinity or selectivity [6, 7]. Consequently, there are a number of different binding modes that can be accommodated within the cavity of I-FABP.

To investigate the possible functional significance of drug binding to I-FABP, we have examined the impact of I-FABP on transmembrane drug transport. In the first instance, drug absorption patterns across the apical enterocyte membrane were modeled by the inclusion or exclusion of I-FABP in the acceptor compartment of in vitro PAMPA assays conducted across a representative phospholipid membrane. In this model, drug movement from the donor to acceptor compartments reflects (i) diffusion across the UWL present on the surface of the membrane in the donor chamber, (ii) partition from the donor compartment (as a surrogate for the GI lumen) into the membrane, (iii) diffusion across the membrane, (iv) partition out of the membrane into the UWL on the acceptor chamber side of the membrane (representing the enterocyte cytosol), and, finally, (v) diffusion across the UWL into the bulk (stirred) environment of the acceptor chamber. Any one of these processes may become rate limiting in terms of overall transport, and the current data suggest that the importance of each is dependent on the physicochemical properties of the drug (primarily lipophilicity), the properties of the fluids in contact with the membrane (and the proteins contained therein), and the nature of the binding interactions that may occur between the drug molecule and the binding proteins in the acceptor (cf. intracellular) compartment (Figure 3).

Uptake from the donor chamber into the membrane (steps i and ii) was essentially a function of drug lipophilicity (Figure 2; Table 2). As such, for the least lipophilic probe (ibuprofen) uptake was poor and essentially the rate-limiting step in terms of transport. In contrast, membrane uptake increased for the more lipophilic compounds and for the most lipophilic (oleic acid, progesterone, diazepam) was rapid and likely limited only by permeability across the UWL (step i). Intermediate uptake was evident for

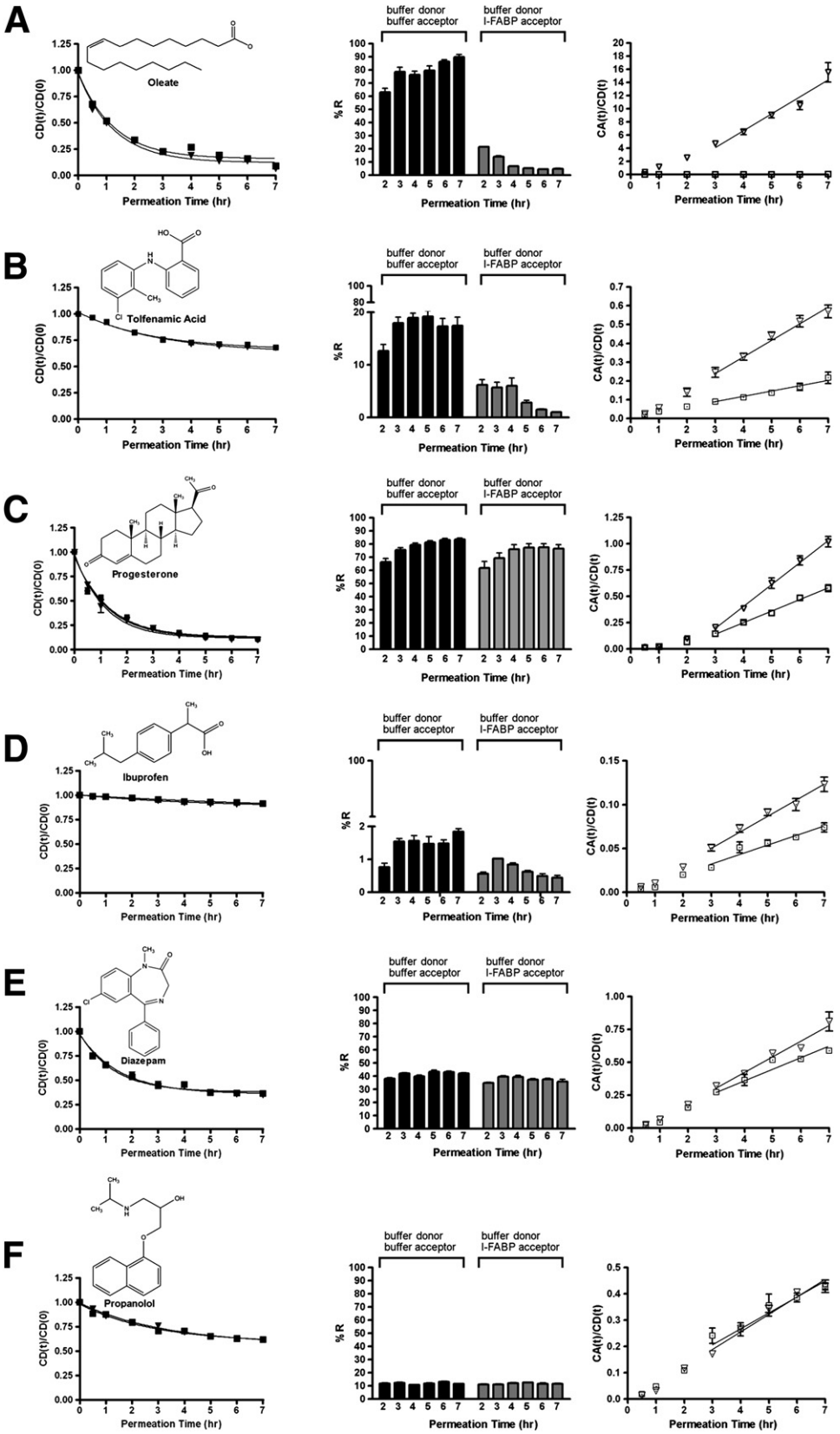
A
Oleate
CD(t)/CD(0)
Permeation Time (hr)
buffer donor
buffer acceptor
buffer donor
I-FABP acceptor
%R
CA(t)/CD(t)
B
Tolfenamic Acid
C
Progesterone
D
Ibuprofen
E
Diazepam
F
Propanolol

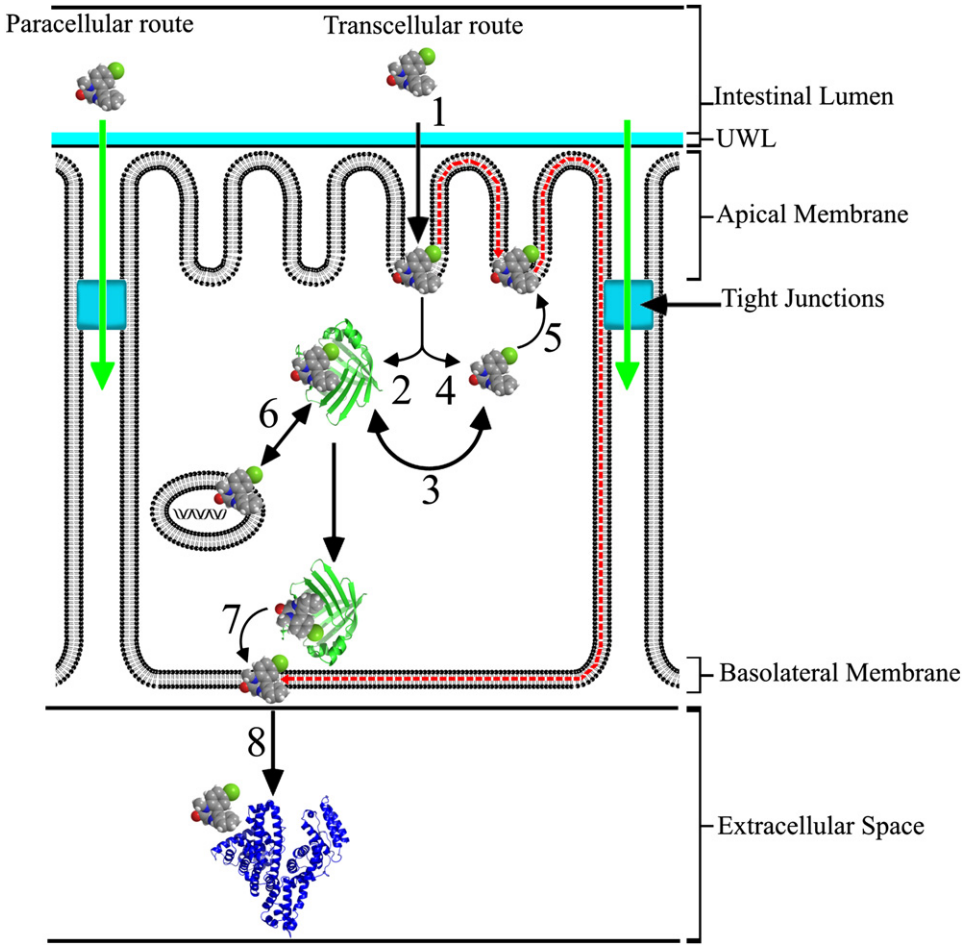

Figure 3. Schematic Representation of Proposed Passive Molecular Transport Mechanisms for a Lipophilic Drug across the Enterocyte

The passive diffusional uptake of a lipophilic drug from the intestinal lumen across the enterocyte interior is initiated by (1) partitioning into the outer leaflet of the apical membrane and movement across the bilayer core. (Active uptake or transport mechanisms within the apical membrane are also present; however, they are omitted for clarity.) Partitioning from the inner leaflet of the apical membrane into the cytosol subsequently occurs where binding to FABP (2) favors cytoplasmic solubilization. Binding to I-FABP in the cytoplasm is a function of the operational dissociation constant (K_d), [free drug] and [*apo*-I-FABP], in the cytosol (3). The high concentration of I-FABP in the enterocyte facilitates binding of lipophilic drugs with moderate affinities. In the absence of FABP (4), diffusional return to the apical membrane is expected to be favored (5). I-FABP binding allows drug access to intracellular organelles such as the nucleus (depicted) (6) and transcellular delivery to the basolateral membrane (7). Uptake from the basolateral membrane into the extracellular space is driven by high-capacity HSA binding (8). The low-capacity paracellular transport route is represented by green arrows and is predominately responsible for the absorption of hydrophilic molecules with limited membrane affinity. The broken, red arrow represents the lateral diffusion pathway of the drug within the plasma membrane.

drugs with intermediate lipophilicity (tolfenamic acid, propranolol). Uptake permeability coefficients were identical regardless of the presence or absence of I-FABP in the acceptor compartment (Table 2). This is consistent with the literature, which suggests that passive membrane permeability is determined in large part by lipophilicity (although this concept has been recently refined to include a realization that the anisotropy of lipid bilayers dictates that some degree of amphiphilicity is also required to promote membrane binding [26]).

Transport of the more lipophilic probes into the acceptor compartment (when the acceptor compartment

Figure 2. Transmembrane Flux of Lipophilic Drugs in the Absence and Presence of I-FABP

(A–F) (A) Oleic acid. (B) Tolfenamic acid. (C) Progesterone. (D) Ibuprofen. (E) Diazepam. (F) Propranolol. First panel: the disappearance kinetics of each compound measured as a function of time. Data are represented as the mass fraction in the donor chamber at time t (CD[t]) relative to time 0 (CD[0]). Middle panel: the percentage membrane retention (%R) of each compound in the absence (black bars) and presence (gray bars) of I-FABP in the acceptor chamber. Third panel: the appearance flux of drug into the acceptor chamber over time in the absence (squares) and presence (triangles) of 0.33 mM I-FABP in the acceptor chamber. Data are mean ($n \geq 3$) ± SE.

contained only buffer) was low, and retention in the membrane was high (Table S1). Since membrane uptake was relatively facile for these compounds and UWL permeability was essentially identical on both sides of the membrane (and relatively high), the rate-limiting steps to transmembrane transport were expected to be either diffusion across the phospholipid bilayer (step iii) or partitioning out of the membrane (step iv) into the aqueous environment of the acceptor chamber. The data presented in the current studies do not distinguish specifically between diffusion across the membrane (step iii), the importance of which in the overall membrane transport of FA remains contentious [27, 28], and dissociation from the membrane into the receptor buffers (step iv). The current data do, however, suggest that significant increases in transport are possible when physiological concentrations of I-FABP are added to the fluids bathing the acceptor side of a model membrane. This is reflective of the situation in vivo in which FA (or lipophilic drugs) within the inner leaflet of the apical membrane of the enterocyte is accessible to intracellular drug-binding proteins, and is also consistent with the suggestion that drug or FA binding to iLBP may facilitate membrane dissociation. The increase in the rate and extent of transport in the current studies was, at least in rank-order terms, reflective of the ligand binding affinity for I-FABP. Thus, effects were especially noticeable for oleic acid (K_i = 0.06 μM), but were also clearly demonstrated with tolfenamic acid (K_i = 2.8 μM), and to a lesser extent progesterone (K_i = 20 μM). Importantly, the cytosolic concentration of FABPs in the enterocyte is 0.2–0.4 mM [1, 3, 4], which is far in excess of the total FA concentration, leaving excess FABP available for binding to lower-affinity ligands, including drug molecules.

While molecular interactions between drug molecules and iLBPs clearly favor drug entry into the enterocyte, it is also apparent that the same interactions may impede drug transport from the cytosol, into and across the basolateral membrane. To assess this issue, an additional series of PAMPA studies was conducted, and the data in Table 3 demonstrate that, in the absence of albumin in the acceptor chamber, the transmembrane transport of oleic acid, tolfenamic acid, and progesterone is indeed impeded by the presence of I-FABP in the donor compartment. However, it is also clear that the presence of albumin in the acceptor compartment dramatically enhances membrane transport, and, again, the degree of enhancement is consistent with drug-protein binding affinity. Similar trends were seen for ibuprofen; however, in this case, the protein-binding response was considerably damped by the intrinsically low membrane permeability of this less lipophilic drug. Diazepam permeability was particularly enhanced by the presence of albumin in the acceptor chamber, a situation reflecting its high affinity for albumin and relatively poor affinity for I-FABP.

The data therefore suggest that the transport of a number of lipophilic drugs across the apical membrane of the enterocyte and into the essentially aqueous environment of the enterocyte cytosol is, in an analogous fashion to oleic acid, facilitated by interaction with a cytosolic binding protein. Numerous experimental and theoretical studies have shown that the presence of FABP stimulates FA mobility in artificial systems [10, 29], cell culture models [30], and perfused rat livers [31]. The current studies demonstrate that several classes of lipophilic drug molecules bind to I-FABP, and that the presence of I-FABP in a model membrane system facilitates their transmembrane transport.

Within the cytosol, iLBPs have also previously been shown to facilitate the delivery of endogenous ligands (FA) to specific intracellular locations, including the endoplasmic reticulum (where re-esterification to triglyceride and subsequent assembly into lipoproteins occurs), and to the nucleus, where FA regulates the expression of a number of proteins involved in lipid metabolism, including FABP, via binding to nuclear hormone receptors (NHRs) such as the PPARs [9, 12, 32]. In the latter case, iLBPs appear to govern the transcriptional activities of their endogenous ligands by targeting them to cognate NHRs, which, in turn, effects transcription of the genes associated with their absorption and metabolism [9, 12, 32]. Previous studies have shown that regulation of numerous proteins, including the cytochrome P450 enzymes and efflux transporters such as p-glycoprotein, involved in detoxification of drug molecules are also under the control of NHRs [33]. Together with the current data, this raises the interesting possibility that iLBPs may also play a role in directing intracellular interactions of drug molecules with NHRs, thereby affecting transcriptional changes to the proteins involved with drug detoxification (Figure 3). Studies to address this latter aspect are ongoing.

SIGNIFICANCE

To our knowledge, this work provides a new level of understanding of the process of drug absorption and the possible mechanisms by which drug molecules are transported across the absorptive cells lining the small intestine (enterocytes) and are delivered to cytosolic sites of metabolism and transcriptional regulation. While there has been considerable recent interest in the role of membrane-resident transporters in the movement of drug molecules across the apical and basolateral membranes of the enterocyte, far less evidence exists to explain the mechanism of transport of drugs across the cellular cytoplasm. This is especially true for very poorly water-soluble and highly lipophilic drugs in which transport across the essentially aqueous domain of the cellular cytoplasm is likely to be limiting. It is well known that families of intracellular binding proteins assist in the movement and delivery of endogenous lipophilic ligands such as FAs to intracellular organelles. To this end, the current study is the first, to our knowledge, to describe the specific binding properties of a range of drug molecules to one of these intracellular carrier proteins (I-FABP), and to link this structural and binding affinity data to a functional outcome, namely, drug transport across a model membrane system.

EXPERIMENTAL PROCEDURES

Materials

Oleic acid, [1-^{14}C] (60 mCi/mmol), and ibuprofen, *R/S*-[carboxylate-^{14}C] (60 mCi/mmol), were purchased from MP Biomedicals Australia (Seven Hills, N.S.W., Australia). Diazepam, [*methyl*-^{3}H] (76 Ci/mmol); propranolol, L-[4-^{3}H] (20 Ci/mmol); ^{14}C-D-mannitol, [1-^{14}C] (56 mCi/mmol); caffeine, [1-*methyl*-^{14}C] (51.2 mCi/mmol); and progesterone, [1,2,6,7-^{3}H(N)] (52 Ci/mmol) were purchased from PerkinElmer Life Sciences (Boston, MA). Isopropyl β-D-thiogalactopyranoside (IPTG) was purchased from BioVectra (Prince Edward Island, Canada). *R*- and *S*-flurbiprofen were purchased from Cayman Chemical Company (Ann Arbor, Michigan). All other (nonradiolabelled) drugs, 1-anilino-8-naphthalene sulfonic acid (ANS), and myristic acid were obtained from Sigma (Sydney, N.S.W., Australia). The MultiScreen Permeability Plate Assembly was purchased from *p*ION, Inc. (Woburn, MA).

Expression and Purification of Rat I-FABP

Recombinant rat I-FABP protein in the unlabelled or ^{15}N/^{13}C-isotopically labeled form was expressed and purified as described previously [11].

Fluorescence Measurements

Drug binding affinity to I-FABP was measured as described previously [11]. Fluorimetric titrations were performed below the aqueous solubility and critical micellular concentration limits of the test compounds. The solubility limits of test compounds in the assay buffer were tested by UV/Vis spectrophotometry. None of the compounds displayed significant absorption in the wavelength region of excitation (400 nm) or emission (420–600 nm); thus, no corrections for inner filter effects were applied. ANS binding and displacement assays for drug binding to human serum albumin (HSA) were as described previously [34]. The dissociation constant of ANS for HSA in buffer A (20 mM Tris [pH 8.0]) was 2.7 ± 0.4 μM. Data were analyzed as previously described [11] with GraphPad Prism V4.0 software (GraphPad Software, San Diego, CA). In accordance with the literature, the binding affinity values for drug-HSA ANS displacement assays are reported as operational constants, as the binding stoichiometry of the drug-HSA complexes is not known [34].

NMR Spectroscopy

NMR experiments were conducted at 22°C in 20 mM MES (pH 5.5), 50 mM NaCl (90% H_2O:10% D_2O) on a Varian UNITY Inova 600 MHz spectrometer equipped with a pulsed-field gradient triple-resonance cryoprobe. Standard triple-resonance experiments [35] (and references therein) were employed to obtain assignment for I-FABP. Experiments were processed with NMRPipe [36] and were analyzed by using SPARKY [37]. Chemical-shift perturbations were calculated by using Equation 1:

$$\Delta\delta = \sqrt{\left(\Delta\delta^{13}C_{\alpha}\right)^2 + \left(\Delta\delta^{13}C_{\beta}\right)^2}, \quad (1)$$

where $\Delta\delta^{13}C_{\alpha}$ and $\Delta\delta^{13}C_{\beta}$, respectively, denote the $^{13}C_{\alpha}$ and $^{13}C_{\beta}$ chemical-shift changes between the apo and holo proteins for a particular residue. A combined chemical-shift change > 0.6 ppm was taken as significant [38]. For palmitic acid, the resonances of Ala32, Phe62, and Ser71 were omitted from the analysis, due to the large deviation of their chemical shifts from average values collated in the BioMagResBank database. Chemical-shift perturbations were mapped onto crystallographic structures of rat I-FABP by using ProtSkin [39], and figures were generated with PYMOL [40].

Chemical Synthesis

Fenofibric acid was prepared by alkaline hydrolysis of fenofibrate under mild conditions as previously described [41].

Molecular Docking

Drug structures were docked into the rat I-FABP crystal structure (1ICM) by using FlexX V1.12 as implemented in Sybyl V6.91 (Tripos Inc., St. Louis, MO).

Chemi-Informatics Calculations

The log P, log D (pH 7.4), and pKa values of the test compounds were calculated by using Advanced Chemistry Development software Solaris V4.67 (ACD/Labs, Toronto, Canada).

Parallel Artificial Membrane Permeability Assay

Filter-immobilized artificial membrane techniques were employed for assessing the membrane transport of drug molecules in the presence and absence of protein acceptor sinks [14, 21, 42]. The parallel artificial membrane permeability assay (PAMPA) consists of a "sandwich" assembly formed from a 96-well microfilter acceptor plate (Millipore Multiscreen, Sydney, N.S.W., Australia) and an indented 96-well filter plate (*p*ION). Each composite well of the assembly is divided into two chambers, a donor at the bottom and an acceptor at the top, separated by a 125 μm thick hydrophobic polyvinylidene fluoride (PVDF) microfilter disc (0.45 μm pore size). The disc of each well is coated with a 2% (w/v) dodecane solution of 1,2-dioleoyl-sn-glycero-3-phosphocholine (*p*ION P/N 110669) that forms multilamellar lipid bilayers inside the filter channels when in contact with an aqueous buffer solution. The donor and acceptor solutions contained an identical buffer composition (buffer B, 20 mM Tris [pH 7.4], 50 mM NaCl). The donor buffer solutions contained 0.009–0.35 μCi radiolabelled test compound, 30 μM unlabelled compound (including < 1% [v/v] DMSO), and, where indicated, 0.33 mM I-FABP. Sample solutions were filtered before use. Acceptor solutions contained buffer B, or where indicated 0.66 mM HSA or 0.33 mM I-FABP in buffer B. The acceptor filter plate was placed on top of the donor plate forming the "sandwich" and incubated for 0.5–7.0 hr in a sealed box under conditions of constant humidity to minimize evaporation. At the appropriate sampling points, the PAMPA sandwich was separated, and the radioactivity in both donor and acceptor compartments was assayed by liquid scintillation counting of 100 μl samples from each chamber. The concentration of drug in each chamber was determined from the specific radioactivity of each compound. Tolfenamic acid transport assays were performed with unlabelled compound. Sample concentrations were assayed by UV/Vis spectrometry (Tolfenamic acid, λ_{max} = 286 nm).

The rate of solute uptake into the membrane was calculated by fitting the disappearance kinetics data to a single-phase exponential decay equation (Equation 2) [42]:

$$CD(t)/CD(0) = (CD[0] - CDss) * \exp(-K * t) + CDss, \quad (2)$$

where CD(t) and CD(0) are the concentrations of compound in the donor chamber at time t and time 0 (mol/l), respectively. CDss is the postequilibrium (3–7 hr) steady-state concentration of drug in the donor chamber. K is the first-order uptake rate constant (mol/l/s). The permeability coefficient (P_e) describing uptake into the membrane was calculated from K by using Equation 3:

$$P_e\left(10^{-6}\ \mathrm{cm/s}\right) = K \times (V_D/A), \quad (3)$$

where VD is the volume in the donor chamber (0.2 cm^3), and A is the effective surface area of the filter disc available for diffusion (0.18 cm^2). The actual filter surface area, 0.24 cm^2, was corrected for an apparent membrane porosity of 76% [21] to give an effective filter surface area of 0.18 cm^2.

P_e describing donor-to-acceptor transmembrane transport was also calculated by using data describing the appearance of radiolabelled compound in the acceptor chamber over time. Permeability coefficients were generated by using Equation 4 and data taken over the period of steady-state transport (which generally occurred over the period of 3–7 hr):

$$P_e\left(10^{-6}\ \mathrm{cm/s}\right) = dCA/dt \times (V_A/A \times CD[0]), \quad (4)$$

where *dCA/dt* is the rate of change in the concentration of drug in the acceptor chamber over the steady-state transport period of 3–7 hr (i.e., the flux into the acceptor chamber, mol/l/s). CD(0) is the initial concentration of compound in the donor chamber at the start of the steady-state transport period (mol/l), V_A is the volume in the acceptor chamber (0.2 cm^3), and A is the effective surface area of the filter disc available for diffusion (0.18 cm^2). All experiments were performed in triplicate, and data are reported as mean ± SD.

Mass balance calculations (Equation 5) were used to quantify the proportion of material retained in the phospholipid membrane barrier (%R) (Equation 6), where CA(t) and CD(t) are the concentration of the compound in the acceptor and donor chambers, respectively, at time (t).

$$\text{Mass balance} = (\text{CA}[t] + \text{CD}[t])/\text{CD}(0), \quad (5)$$

$$\%\text{R} = (1 - \text{Mass balance}) \times 100. \quad (6)$$

Statistically significant differences between data sets were determined by one-way ANOVA, followed by Tukey's test for multiple comparisons at a significance level of $\alpha = 0.05$. All statistical analysis was performed by using GraphPad Prism V4.0 software.

Supplemental Data

Supplemental data include additional analysis of the membrane retention data for the PAMPA drug transport model, chemical structures of the drugs examined for I-FABP binding affinity, and ^{1}H-^{15}N HSQC spectra of drug-I-FABP complexes are available online at http://www.chembiol.com/cgi/content/full/14/4/453/DC1/.

ACKNOWLEDGMENTS

We thank Mrs. Anna Velkov for assistance with preparation of the manuscript. T.V. is the recipient of a Fellowship (384300) from the National Health and Medical Research Council of Australia. This work was supported by grants from the Australian Research Council (DP0342458, DP0664069).

Received: June 20, 2006
Revised: March 2, 2007
Accepted: March 7, 2007
Published: April 27, 2007

REFERENCES

1. Glatz, J.F.C., Van der Vusse, G.J., and Veerkamp, J.H. (1988). Fatty acid binding proteins and their physiological significance. News Physiol. Sci. *35*, 41–43.
2. Hertzel, A.V., and Bernlohr, D.A. (2000). The mammalian fatty acid-binding protein multigene family: molecular and genetic insights into function. Trends Endocrinol. Metab. *5*, 175–179.
3. Paulussen, R.J., Van Moerkerk, H.T., and Veerkamp, J.H. (1990). Immunochemical quantitation of fatty acid-binding proteins. Tissue distribution of liver and heart FABP types in human and porcine tissues. Int. J. Biochem. *22*, 393–398.
4. Bass, N.M., and Manning, J.A. (1986). Tissue expression of three structurally different fatty acid binding proteins from rat heart muscle, liver, and intestine. Biochem. Biophys. Res. Commun. *137*, 929–935.
5. Hodsdon, M.E., and Cistola, D.P. (1997). Discrete backbone disorder in the nuclear magnetic resonance structure of apo intestinal fatty acid-binding protein: implications for the mechanism of ligand entry. Biochemistry *36*, 1450–1460.
6. Zhang, F., Lucke, C., Baier, L.J., Sacchettini, J.C., and Hamilton, J.A. (1997). Solution structure of human intestinal fatty acid binding protein: implications for ligand entry and exit. J. Biomol. NMR *9*, 213–228.
7. Zhang, F., Lucke, C., Baier, L.J., Sacchettini, J.C., and Hamilton, J.A. (2003). Solution structure of human intestinal fatty acid binding protein with a naturally-occurring single amino acid substitution (A54T) that is associated with altered lipid metabolism. Biochemistry *42*, 7339–7347.
8. Thompson, J., Winter, N., Terwey, D., Bratt, J., and Banaszak, L. (1997). The crystal structure of the liver fatty acid-binding protein. A complex with two bound oleates. J. Biol. Chem. *272*, 7140–7150.
9. Coe, N.R., and Bernlohr, D.A. (1998). Physiological properties and functions of intracellular fatty acid-binding proteins. Biochim. Biophys. Acta *1391*, 287–306.
10. Storch, J., Veerkamp, J.H., and Hsu, K.T. (2002). Similar mechanisms of fatty acid transfer from human and rodent fatty acid-binding proteins to membranes: liver, intestine, heart muscle, and adipose tissue FABPs. Mol. Cell. Biochem. *239*, 25–33.
11. Velkov, T., Chuang, S., Wielens, J., Sakellaris, H., Charman, W.N., Porter, C.J., and Scanlon, M.J. (2005). The interaction of lipophilic drugs with intestinal fatty acid-binding protein. J. Biol. Chem. *280*, 17769–17776.
12. Wolfrum, C., Borrmann, C.M., Borchers, T., and Spener, F. (2001). Fatty acids and hypolipidemic drugs regulate peroxisome proliferator-activated receptors α- and γ-mediated gene expression via liver fatty acid binding protein: a signaling path to the nucleus. Proc. Natl. Acad. Sci. USA *98*, 2323–2328.
13. Artursson, P., Palm, K., and Luthman, K. (2001). Caco-2 monolayers in experimental and theoretical predictions of drug transport. Adv. Drug Deliv. Rev. *46*, 27–43.
14. Avdeef, A. (2003). Drug Bioavailability: Estimation of Solubility, Permeability, Absorption and Bioavailability (Weinheim, Germany: Wiley-VCH).
15. Ito, K., Suzuki, H., Horie, T., and Sugiyama, Y. (2005). Apical/basolateral surface expression of drug transporters and its role in vectorial drug transport. Pharm. Res. *22*, 1559–1577.
16. Ory, J.J., and Banaszak, L.J. (1999). Studies of the ligand binding reaction of adipocyte lipid binding protein using the fluorescent probe 1, 8-anilinonaphthalene-8-sulfonate. Biophys. J. *77*, 1107–1116.
17. Hodsdon, M.E., Ponder, J.W., and Cistola, D.P. (1996). The NMR solution structure of intestinal fatty acid-binding protein complexed with palmitate: application of a novel distance geometry algorithm. J. Mol. Biol. *264*, 585–602.
18. Grzesiek, S., Bax, A., Clore, G.M., Gronenborn, A.M., Hu, J.S., Kaufman, J., Palmer, I., Stahl, S.J., and Wingfield, P.T. (1996). The solution structure of HIV-1 Nef reveals an unexpected fold and permits delineation of the binding surface for the SH3 domain of Hck tyrosine protein kinase. Nat. Struct. Biol. *3*, 340–345.
19. Sacchettini, J.C., Gordon, J.I., and Banaszak, L.J. (1989). Crystal structure of rat intestinal fatty-acid-binding protein. Refinement and analysis of the *Escherichia coli*-derived protein with bound palmitate. J. Mol. Biol. *208*, 327–339.
20. Peters, T., Jr. (1996). All about Albumin: Biochemistry, Genetics, and Medical Applications (San Diego: Academic Press).
21. Ruell, J.A., and Avdeef, A. (2004). Absorption screening using the PAMPA approach. In Methods in Pharmacology and Toxicology Optimization in Drug Discovery: In Vitro Methods, Z. Yan and G.W. Caldwell, eds. (Totowa, NJ: Humana Press), pp. 36–87.
22. Sawada, G.A., Barsuhn, C.L., Lutzke, B.S., Houghton, M.E., Padbury, G.E., Ho, N.F., and Raub, T.J. (1999). Increased lipophilicity and subsequent cell partitioning decrease passive transcellular diffusion of novel, highly lipophilic antioxidants. J. Pharmacol. Exp. Ther. *288*, 1317–1326.
23. Lucke, C., Gutiérrez-González, L.H., and Hamilton, J. (2003). Intracellular lipid binding proteins: evolution, structure and ligand binding. In Cellular Proteins and their Fatty Acids in Health and

Disease, A.K. Duttaroy and F. Spener, eds. (Weinheim, Germany: Wiley-VCH), pp. 95–118.

24. Sacchettini, J.C., and Gordon, J.I. (1993). Rat intestinal fatty acid binding protein. A model system for analyzing the forces that can bind fatty acids to proteins. J. Biol. Chem. *268*, 18399–18402.
25. Kirk, W.R., Kurian, E., and Prendergast, F.G. (1996). Characterization of the sources of protein-ligand affinity: 1-sulfonato-8-(1′)anilinonaphthalene binding to intestinal fatty acid binding protein. Biophys. J. *70*, 69–83.
26. Fischer, H., Gottschlich, R., and Seelig, A. (1998). Blood-brain barrier permeation: molecular parameters governing passive diffusion. J. Membr. Biol. *165*, 201–211.
27. Kampf, J.P., Cupp, D., and Kleinfeld, A.M. (2006). Different mechanisms of free fatty acid flip-flop and dissociation revealed by temperature and molecular species dependence of transport across lipid vesicles. J. Biol. Chem. *281*, 21566–21574.
28. Guo, W., Huang, N., Cai, J., Xie, W., and Hamilton, J.A. (2006). Fatty acid transport and metabolism in HepG2 cells. Am. J. Physiol. Gastrointest. Liver Physiol. *290*, G528–G534.
29. Weisiger, R.A., and Zucker, S.D. (2002). Transfer of fatty acids between intracellular membranes: roles of soluble binding proteins, distance, and time. Am. J. Physiol. Gastrointest. Liver Physiol. *282*, G105–G115.
30. Trotter, P.J., and Storch, J. (1991). Fatty acid uptake and metabolism in a human intestinal cell line (Caco-2): comparison of apical and basolateral incubation. J. Lipid Res. *32*, 293–304.
31. Luxon, B.A., Milliano, M.T., and Weisiger, R.A. (2000). Induction of hepatic cytosolic fatty acid binding protein with clofibrate accelerates both membrane and cytoplasmic transport of palmitate. Biochim. Biophys. Acta *1487*, 309–318.
32. Adida, A., and Spener, F. (2006). Adipocyte-type fatty acid-binding protein as inter-compartmental shuttle for peroxisome proliferator activated receptor γ agonists in cultured cell. Biochim. Biophys. Acta *1761*, 172–181.
33. Synold, T.W., Dussault, I., and Forman, B.M. (2001). The orphan nuclear receptor SXR coordinately regulates drug metabolism and transport. Nat. Med. *7*, 584–590.
34. Bagatolli, L.A., Kivatinitz, S.C., and Fidelio, G.D. (1996). Interaction of small ligands with human serum albumin IIIA subdomain. How to determine the affinity constant using an easy steady state fluorescent method. J. Pharm. Sci. *85*, 1131–1132.
35. Grzesiek, S., and Bax, A. (1992). Improved 3D triple-resonance NMR techniques applied to a 31-kDa protein. J. Magn. Reson. *96*, 432–440.
36. Delaglio, F., Grzesiek, S., Vuister, G.W., Zhu, G., Pfeifer, J., and Bax, A. (1995). NMRPipe: a multidimensional spectral processing system based on UNIX pipes. J. Biolmol. NMR *6*, 277–293.
37. Goddard, T.D., and Kneller, D.G. (2006). SPARKY 3 (http://www.cgl.ucsf.edu/home/sparky).
38. Tugarinov, V., and Kay, L.E. (2003). Quantitative NMR studies of high molecular weight proteins: application to domain orientation and ligand binding in the 723 residue enzyme malate synthase G. J. Mol. Biol. *327*, 1121–1133.
39. Deprez, C., Lloubes, R., Gavioli, M., Marion, D., Guerlesquin, F., and Blanchard, L. (2005). Solution structure of the *E. coli* TolA C-terminal domain reveals conformational changes upon binding to the phage g3p N-terminal domain. J. Mol. Biol. *346*, 1047–1057.
40. DeLano, W.L. (2002). PyMol (http://www.pymol.org).
41. Rath, N.P., Haq, W., and Balendiran, G.K. (2005). Fenofibric acid. Acta Crystallogr. C *61*, o81–o84.
42. Avdeef, A. (2003). Absorption and Drug Development Solubility, Permeability, and Charge State (Hoboken, NJ: Wiley-Interscience).

Accession Numbers

$^{13}C_{\alpha}$ and $^{13}C_{\beta}$ chemical-shift assignments for drug-I-FABP complexes have been deposited at BioMagResBank (http://www.bmrb.wisc.edu) with Accession Numbers 15082, 7356, 7357, and 7355.